Scheme I

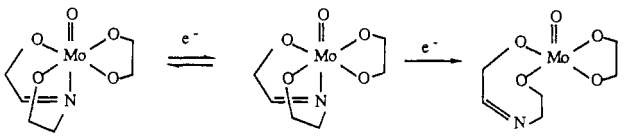

The reversible $Mo^{VI/V}$ electrochemistry exhibited by these six-coordinate MoO^{4+} complexes contrasts dramatically with the behavior of this functional group in a seven-coordinate environment.[12] Irreversible electrochemistry at seven-coordinate MoO^{4+} centers results from the fact that the four Mo d_{xy} orbital lobes that become singly occupied upon reduction to Mo(V) experience unfavorable interactions with the five equatorial bonds present in the pentagonal-bipyramidal geometry and initiate metal-ligand bond cleavage reactions during charge transfer. Preparation and structural characterization of six-coordinate MoO(cat)(Sap) complexes demonstrates that when only four bonds are present in the equatorial plane, these unfavorable interactions are absent and reversible one-electron electrochemistry prevails. The six-coordinate distorted-octahedral geometry of MoO(Naphcat)(Sap) is characteristic also of monooxomolybdenum(V) (MoO^{3+}) complexes,[2a,32] consequently we expect that Mo(VI) to Mo(V) reduction of MoO(cat)(Sap) proceeds with minimal structural change as shown in the first step of Scheme I.

Figure 5a shows that the second reduction of MoO(Cat)(Sap) (eq 6) is irreversible at a sweep rate of 0.2 V s^{-1}. The voltammetric peak widths ($E_p - E_{p/2}$ = 70-110 mV) and shifts in voltammetric peak potential with sweep rate ($\Delta E_p/\Delta(\log v)$ = 55-70 mV) are consistent with slow heterogeneous charge transfer.[33] Thus, we conclude that a change in structure accompanies reduction of Mo(V) to Mo(IV). Since monooxomolybdenum(IV) most commonly exists in a five-coordinate square-pyramidal environment[34] and structural constraints involving the Mo-N bond in MoO(Naphcat)(Sap) have been noted earlier, a probable structural change is displacement of the Schiff base N atom trans to terminal oxo as shown in the second half of Scheme I.

Figure 5 further shows that the second MoO(Cat)(Sap) reduction wave experiences a transition from irreversible to quasireversible behavior as the sweep rate is reduced from 200 to 50 mV s^{-1}. All three MoO(cat)(Sap) complexes exhibit a similar anodic peak at sweep rates below 0.1 Vs^{-1}. This unusual observation suggests that a slow chemical reaction takes place following irreversible Mo(V) reduction, which facilitates Mo(IV) oxidation on the positive sweep. A possible explanation of this behavior is reattachment of the Schiff base N atom to Mo (possibly in a different configuration) via a process conceptually similar to the base-on/base-off reactions associated with the cobalt-centered electrochemistry of vitamin B-12 derivatives.[35] A considerable activation energy barrier must be associated with this process because it occurs at a relatively slow rate and results in large separations between the anodic and cathodic peak potentials. (ΔE_p = 150-200 mV at v = 0.05 V s^{-1}).

Acknowledgment. We wish to acknowledge financial support from the National Science Foundation (Grant No. CHE-87-18013, F.A.S.) and the National Institutes of Health (Grant No. GM-38401-16, W.R.S.). We thank Dr. J. W. Louda (Florida Atlantic University) and Professor John H. Enemark and M. LeBarre (University of Arizona) for obtaining and providing assistance in interpreting mass and ^{95}Mo NMR spectra, respectively.

Supplementary Material Available: Table SI, anisotropic thermal parameters for MoO(Naphcat)(Sap), and Table SII, fixed hydrogen atom coordinates (3 pages); a listing of observed and calculated structure factor amplitudes (×10) (20 pages). Ordering information is given on any current masthead page.

(32) Cleland, W. E., Jr.; Barnhart, K. M.; Yamanouchi, K.; Collison, D.; Mabbs, F. E.; Ortega, R. G.; Enemark, J. H. *Inorg. Chem.* **1987**, *26*, 1017.
(33) Nicholson, R. S.; Shain, I. *Anal. Chem.* **1964**, *36*, 706.
(34) Stiefel, E. I. *Prog. Inorg. Chem.* **1977**, *22*, 1.
(35) Lexa, D.; Saveant, J. M. *Acc. Chem. Res.* **1983**, *16*, 235.

Contribution from the Laboratoire de Chimie des Organométalliques associé au CNRS (UA 415), Université de Rennes I, 35042 Rennes Cedex, France

Synthesis and Proton NMR Studies of the Electronic Structure of Ferric Phosphine Porphyrin Complexes

G. Simonneaux* and P. Sodano

Received April 14, 1988

The preparation and spectral properties of low-spin ferric phosphine complexes of a series of synthetic and natural porphyrins have been reported. The proton NMR spectra of $Fe(TPP)(PMe_3)_2ClO_4$ and $Fe(TPP)(PMe_3)(1\text{-MeIm})ClO_4$ have been analyzed. The axial ligand hyperfine shifts have been separated into their dipolar and contact contributions by using both the dominant dipolar shifts for certain porphyrin positions and the magnetic anisotropy data derived from low-temperature ESR spectra. The contact shifts are shown to arise primarily from iron → phosphine π^* charge transfer. The trimethylphosphine H peak is shown to shift characteristically upfield on going from $[Fe(TPP)(PMe_3)_2]^+$ to $[Fe(TPP)(PMe_3)(1\text{-MeIm})]^+$, confirming that this resonance may serve as a new probe for hemoproteins.

Recent investigations in this laboratory have focused on phosphorus-ligated hemoprotein complexes.[1-3] ^1H and ^{31}P NMR techniques have been used to probe the size of the ligand-binding pocket in hemoglobins (Hb) and myoglobin (Mb). The ligand used is a phosphine, PMe_3, which is small enough to complex Hb. In particular, we reported new and definite evidence on direct observation of intermediate ligation states of hemoglobin based on ^{31}P NMR spectra of partially ligated $HbPMe_3$.[4]

Phosphines serve also as useful probes of ferric hemoprotein electronic and molecular structures in part through generation

(1) Bondon, A.; Petrinko, P.; Sodano, P.; Simonneaux, G. *Biochim. Biophys. Acta* **1986**, *872*, 163.
(2) Bondon, A.; Sodano, P.; Simonneaux, G.; Craescu, C. T. *Biochim. Biophys. Acta* **1987**, *914*, 289.
(3) Simonneaux, G.; Bondon, A.; Sodano, P. *Inorg. Chem.* **1987**, *26*, 3636.
(4) Simonneaux, G.; Bondon, A.; Brunel, C.; Sodano, P. *J. Am. Chem. Soc.*, in press.

0020-1669/88/1327-3956$01.50/0

of optical spectra that reflect the nature of the heme trans amino acid.[5] For example, it is interesting to note that phosphines are the only sixth ligand besides mercaptides that produce a clear hyperporphyrin spectrum with oxidized cytochrome P450.[6] We recently reported studies on ^1H paramagnetic shifts of the iron-bound PMe_3 in low-spin ferric complexes of various hemoglobins.[3] It was found that these phosphines, being considerably bulkier than O_2 and CO, can serve as sensitive "steric" probes of the ligand binding in the ferric state since the proton resonances for PMe_3 bound to metHb and metMb were also well separated from the envelope of protein resonances.[3]

In order to improve our understanding of the electron structure of phosphine-ligated hemoproteins, we have herein analyzed the proton NMR spectra of low-spin ferric porphyrin complexes with tertiary phosphines. Previous studies[5,6] on model complexes have been undertaken on dissolved species, and surprisingly there are, to our knowledge, no published reports on the preparation of solid (phosphine)(porphyrinato)iron(III) derivatives.

Experimental Section

As a precaution against the formation of the μ-oxo dimer $[Fe(TPP)]_2O$[8] all reactions were carried out in dried solvents in Schlenk tubes under an Ar or N_2 atmosphere. Solvents were distilled from appropriate drying agents and stored under nitrogen. IR spectra were recorded on a Unicam SP 1100 infrared spectrophotometer. Ultraviolet–visible spectra were recorded with a Jobin Yvon Hitachi spectrophotometer. The ^1H NMR spectra were recorded in a pulse Fourier transform mode with a Bruker AM 300 WB spectrometer. Tetramethylsilane was used as internal reference (solvent CD_2Cl_2). The temperatures are given within 1 K. ESR spectra were recorded at 140 K in frozen solution ($[Fe^{III}]$ = 0.03 M, CH_2Cl_2) with a JEOL spectrometer operating at X-band equipped with a nitrogen low-temperature device. The g values were measured with respect to that of diphenylpicrylhadrazyl (g = 2.0036 ± 0.0003).

Elemental analyses were performed by the Service Central of Analyses (CNRS) at Vernaison, France.

Caution! We have not observed detonation of iron porphyrin perchlorates under our conditions, but care is urged.

Reagents. The following iron porphyrins[9] were prepared by literature methods: $Fe(TPP)ClO_4$,[10] $[Fe(T(m\text{-}Me)PP)]ClO_4$,[11] $Fe[T(p\text{-}Me)PP]ClO_4$,[11] $Fe(DPDME)ClO_4$,[11] $Fe(TPP)(1\text{-}MeIm)_2ClO_4$,[10] and $Fe(TPP)(py)_2ClO_4$.[10]

PMe_3 and PMe_2Ph are commercially available (Strem Chemicals, Inc.).

Synthesis. $Fe(TPP)(PMe_3)_2ClO_4$. To a solution of 0.2 g (0.26 mmol) of $Fe(TPP)ClO_4$ in 20 mL of toluene was added 2.5 equiv of PMe_3 by a syringe at room temperature. The solution was set aside overnight for crystallization. Fine crystals of $Fe(TPP)(PMe_3)_2ClO_4$ were collected by filtration and washed with hexane. Recrystallization was achieved by dissolving the product in a minimum of CH_2Cl_2 (10 mL) and adding hexane (20 mL). The yield was 0.21 g (88%). Anal. Calcd for $C_{50}H_{46}N_4O_4P_2ClFe$: C, 65.20; H, 5.0; N, 6.09; P, 6.74. Found: C, 65.11; H, 5.34; N, 5.72; P, 6.40. UV–vis (λ_{max}, nm (ϵ, mM^{-1} cm^{-1}); CH_2Cl_2): 359 (99), 440 (128), 618 (45).

The trimethylphosphine derivatives of $Fe[T(m\text{-}Me)PP]ClO_4$, $Fe[T(p\text{-}Me)PP]ClO_4$, and $Fe(TPP)(PMe_2Ph)_2ClO_4$ were prepared as described above. The products were not recrystallized and were characterized by NMR and UV–visible spectroscopy. UV–vis (λ_{max}, nm (ϵ, mM^{-1} cm^{-1}); CH_2Cl_2): $Fe[T(m\text{-}Me)PP](PMe_3)_2ClO_4$, 359, 440, 619; $Fe[T(p\text{-}Me)PP](PMe_3)_2ClO_4$, 360, 441, 618; $Fe(TPP)(PMe_2Ph)_2ClO_4$, 363 (105), 442 (114), 619 (52). ^1H NMR (ppm): PMe_2Ph, −4.1 (Me), 6.53 and 12.3 (o + m), 9.71 (p); porphyrin, −20.05 (pyrr), 6.80 (m), 6.33 (p), 5 (o).

$Fe(TPP)(PMe_3)(1\text{-}MeIm)ClO_4\cdot CH_2Cl_2$. To a solution of $Fe(TPP)(1\text{-}MeIm)_2ClO_4$ (0.3 g, 0.32 mmol), 1-MeIm (2 equiv), and CH_2Cl_2 (15 mL) was added gradually 1.2 equiv of PMe_3 in 5 mL of CH_2Cl_2. The solution was stirred for 10 min. After addition of 40 mL of hexane, crystals were collected by filtration and washed with hexane. The yield of CH_2Cl_2 solvate was 0.25 g (78%). Anal. Calcd for $C_{52}H_{45}N_6O_4PCl_3Fe$: C, 61.63; H, 4.44 N, 8.30; P, 3.66. Found: C, 61.74; H, 4.74; N, 8.43; P, 3.69. UV–vis (λ_{max}, nm (ϵ, mM^{-1} cm^{-1}); CH_2Cl_2): 421 (131), 541 (47), 568 (46).

$Fe(TPP)(PMe_3)(py)ClO_4$. This was prepared in a similar manner with $Fe(TPP)(py)_2ClO_4$[10] as the intermediate complex except that this bis(pyridine) adduct was not isolated. The product was not recrystallized prior to spectral determination and was characterized by NMR and UV–visible spectra (75% yield). UV–vis (λ_{max}, nm (ϵ, mM^{-1} cm^{-1}); CH_2Cl_2): 422 (130), 546 (35), 579 (34).

$Fe(DPDME)(PMe_3)_2ClO_4$. The perchlorate derivative of Fe(DPDME) was prepared by silver perchlorate reaction with the corresponding chloride analogue in THF solvent.[10] The product was not recrystallized. Addition of 3 equiv of PMe_3 to this complex (0.2 g) in 20 mL of THF at room temperature gave rapidly the expected product $Fe(DPDME)(PMe_3)_2ClO_4$ with hexane. Entirely satisfactory carbon elemental analyses were not obtained, possibly because of partial contamination with starting materials. UV–vis (λ_{max}, nm; THF): 358, 434, 358. ^1H NMR ($CDCl_3$, ppm): −5.5 (PMe_3); −20.8, −21.9 (pyrr); 23.1, 20, 19.75, 18.8 (CH_3, ring); 10.8 (α-CH_2); 3.5 (ester) (meso H and β-CH_2 were not identified).

$Fe(DPDME)(PMe_3)(1\text{-}MeIm)ClO_4$. A mixture of $Fe(DPDME)ClO_4$ (0.2 g, 0.30 mmol), 1-MeIm (3 equiv), and CH_2Cl_2 (10 mL) was stirred gently for 10 min at room temperature, and then 1.2 equiv of PMe_3 was added with a syringe. Hexane (20 mL) was added gradually, the mixture was set aside overnight for crystallization. Fine crystals of the product were collected by filtration. Recrystallization was achieved by redissolving the product in CH_2Cl_2 (8 mL) and adding 20 mL of hexane. The yield was 0.18 g (73%). Anal. Calcd for $C_{37}H_{45}N_6O_8PClFe$: C, 54.1; H, 5.2; N, 10.25; P, 3.73. Found: C, 54.7; H, 5.56; N, 10.28; P, 3.43. UV–vis (λ_{max}, nm (ϵ, mM^{-1} cm^{-1}); CH_2Cl_2): 343 (69), 411 (129), 523 (36). ^1H NMR (CD_2Cl_2, ppm): −13.2 (PMe_3); 14.5 (CH_3, 1-MeIm); −19.6, −12.5 (pyrr); 20.6, 18, 17.1, 16.8 (CH_3, ring); 12 (α-CH_2); 3.5 (CH_3, ester).

Table I. Observed Shifts and Separation of the Isotropic Shift into Contact and Dipolar Contributions in $Fe(TPP)(PMe_3)_2ClO_4$

proton type	$\Delta H/H^a$	$(\Delta H/H)_{iso}{}^b$	$(\Delta H_c/H)_{dip}$ A[c]	$(\Delta H_c/H)_{dip}$ B[d]	$(\Delta H/H)_{con}$ A	$(\Delta H/H)_{con}$ B
o-H	5.00	−2.91	−2.91	−2.16	0	−0.75
m-H	6.78	−0.75	−1.32	−0.92	+0.57	+0.23
	(1.7)[e]	(−0.85)		(−0.64)		(−0.21)
p-H	6.36	−1.17	−1.18	−0.82	0	−0.29
	(2.05)[f]	(−0.54)		(−0.68)		(−0.14)
pyrr H	−19.6	−27.81	−5.49	−4.08	−22.32	−23.73
PMe_3	−5.00	−2.39	+14.72	+10.93	−17.11	−13.32

[a] Chemical shifts in ppm at 30 °C with Me_4Si as internal reference. [b] Isotropic shift with the diamagnetic $Fe(TPP)(PMe_3)_2$ complex as reference.[7] [c] Based on relative geometric factors $(3(\cos^2\theta) - 1)/r^3$ and ref 15 (the meso-phenyl shifts are totally dipolar in origin). [d] Based on g values. [e] m-CH_3 shift in parentheses. [f] p-CH_3 shift in parentheses.

Results

Synthesis. A major difficulty that we have encountered in preparing phosphine ferric porphyrin derivatives has been the autoreduction of ferric porphyrins.[12] In the preparation of the axially symmetric $[Fe(P)(PR_3)_2]^+$ derivatives (P = TPP, DPDME),[9] this difficulty has been circumvented by using $Fe(P)ClO_4$ complexes[10,11] as starting materials. Addition under argon of 2 equiv of trimethylphosphine to $Fe(TPP)ClO_4$[10] in toluene affords a high yield of the hexacoordinated complex $Fe(TPP)(PMe_3)_2ClO_4$ (**1**) (Table I). For the preparation of the other symmetric complex $Fe(TPP)(PMe_2Ph)_2ClO_4$, with PMe_2Ph, the same procedure can be used. Mixed-coordinate complexes with TPP have been prepared by addition of 1 equiv of trimethylphosphine to $Fe(TPP)(base)_2ClO_4$ (base = 1-methylimidazole, pyridine)[10] in the presence of an excess of base at room tem-

(5) (a) Ruf, H. H.; Wende, P.; Ullrich, V. *J. Inorg. Biochem.* **1979**, *11*, 189. (b) Ruf, H. H.; Wende, P. *J. Am. Chem. Soc.* **1977**, *99*, 5499.
(6) Mansuy, D.; Duppel, W.; Ruf, H. H.; Ullrich, V. *Hoppe-Seyler's Z. Physiol. Chem.* **1974**, *355*, 1349.
(7) We have previously reported an X-ray structure analysis of an analogous ferrous derivative; see: Sodano, P.; Simonneaux, G. *J. Chem. Soc., Dalton Trans.*, in press.
(8) Fleisher, E. B.; Palmer, J. M.; Srivastava, T. S.; Chatterjee, A. *J. Am. Chem. Soc.* **1971**, *93*, 3162.
(9) Abbreviations used: P, any porphyrin; $(TPP)H_2$, tetraphenylporphyrin; $[T(m\text{-}Me)PP]H_2$, tetrakis(*m*-methylphenyl)porphyrin; $[T(p\text{-}Me)PP]H_2$, tetrakis(*p*-methylphenyl)porphyrin; DPDME, deuteroporphyrin dimethyl ester; 1-MeIm, 1-methylimidazole; Im, imidazole; py, pyridine.
(10) Reed, C. A.; Mashiko, T.; Bentley, S. P.; Kastner, M. E.; Scheidt, W. R.; Spartalian, K.; Lang, G. *J. Am. Chem. Soc.* **1979**, *101*, 2948.
(11) Goff, H.; Shimomura, E. *J. Am. Chem. Soc.* **1980**, *102*, 31.
(12) La Mar, G.; Del Gaudio, J. *Bioinorg. Chem.* **1977**, *2*, 207.

Table II. Observed Shifts and Separation of the Isotropic Shift into Contact and Dipolar Contributions in Fe(TPP)(PMe_3)(1-MeIm)ClO_4

proton type	$\Delta H/H$[a]	$(\Delta H/H)_{iso}$[b]	$(\Delta H/H)_{dip}$ A[c]	$(\Delta H/H)_{dip}$ B[d]	$(\Delta H/H)_{con}$ A	$(\Delta H/H)_{con}$ B
o-H	5.03	−2.75	−2.75	−2.77	0	0
m-H	6.26	−1.23	−1.23	−1.26	0	0
p-H	6.2	−1.23	−1.12	−1.13	~0	~0
pyrr H	−19.45	−27.34	−5.19	−5.24	−22.15	−22.10
PMe_3	−12.95	−10.08	13.92	14.05	−24	−24.10
Me (Im)	15.03	13.43[e]	6.06	6.12	7.37	7.31
CH (Im)	12.18					
	−4.99					
	−15.72					

[a] Chemical shifts in ppm at 30 °C with Me_4Si as internal reference. [b] Isotropic shift with the diamagnetic Fe(TPP)(PMe_3)(1-MeIm) complex as reference.[7] [c] Based on relative geometric factors $(3(\cos^2\theta) - 1)/r^3$ and ref 15. [d] Based on g values. [e] Isotropic shift with the diamagnetic Fe(TPP)(1-MeIm)$_2$ complex.[19]

Table III. Observed Shifts and Separation of the Isotropic Shift into Contact and Dipolar Contributions in Fe(TPP)(PMe_3)(py)ClO_4

proton type	$\Delta H/H$[a]	$(\Delta H/H)_{iso}$[b]	$(\Delta H/H)_{dip}$ A[c]	$(\Delta H/H)_{con}$ A
o-H	5.00	−2.41	−2.41	0
m-H	6.30	−0.96	−1.09	0
p-H	6.30	−0.96	−0.98	0
pyrr H	−20.41	−28.81	−4.55	−24.25
PMe_3	−14.87	−11.94	12.19	−24.13

[a] Chemical shifts in ppm at 30 °C with Me_4Si as internal reference. (Resonances due to the axial pyridine are not assigned.) [b] Isotropic shift with diamagnetic Fe(TPP)(PMe_3)(py) complex as reference.[7] [c] Based on relative geometric factors $(3(\cos^2\theta) - 1)/r^3$ and ref 15.

perature under argon. Such a preparation allows the respective formation of Fe(TPP)(PMe_3)(1-MeIm)ClO_4 (**2**) and Fe(TPP)(PMe_3)(py)ClO_4 (**3**), which have been characterized by UV–visible spectra and ^1H NMR spectroscopy (Tables II and III).

The above-described methods are general and have been used for the preparation of Fe(DPDME)(PMe_3)$_2ClO_4$ and Fe(DPDME)(PMe_3)(1-MeIm)ClO_4. These low-spin complexes have been identified by visible spectra and ^1H NMR spectroscopy (see Experimental Section).

Electronic Spectroscopy. The Fe(TPP)(PR_3)$_2ClO_4$ (PR_3 = PMe_3, PMe_2Ph) complexes exhibited hyperspectra with two Soret bands, one in the 440-nm region and the second in the near-ultraviolet region (360 nm). Phosphine low-spin iron(III) tetraphenylporphyrins with nitrogenous bases exhibited normal porpyrin spectra[13] with one Soret band, although it was red-shifted to 430 nm. It is interesting to note that two phosphines are also necessary for the hyperporphyrin spectrum in the ferrous state with similar models. Hyperporphyrin spectra were also previously reported[7,14] by Ruf et al.[5] for dimercaptide hemin and mercaptide phosphine hemin complexes.

^1H NMR Spectroscopy. The ^1H NMR spectrum of Fe(TPP)(PMe_3)$_2ClO_4$ (**1**) is shown in Figure 1a. The signal in a far-highfield position logically belongs to pyrrole proton atoms on the basis of assignments for low-spin iron(III) porphyrin complexes.[15] The PMe_3 signal is directly assigned through examination of the $P(CD_3)_3$[16] complex ($\delta = -5.0$). Assignment of phenyl signals was possible through examination of *m*- and *p*-methyl TPP complexes in combination with proton-coupled and proton-decoupled experiments. Chemical shift values for meta and para protons and attached methyl groups are listed in Table I.

The ^1H NMR spectrum of Fe(TPP)(PMe_3)(1-MeIm)ClO_4 is shown in Figure 1b. Assignment of PMe_3 ($\delta = -12.95$) was made

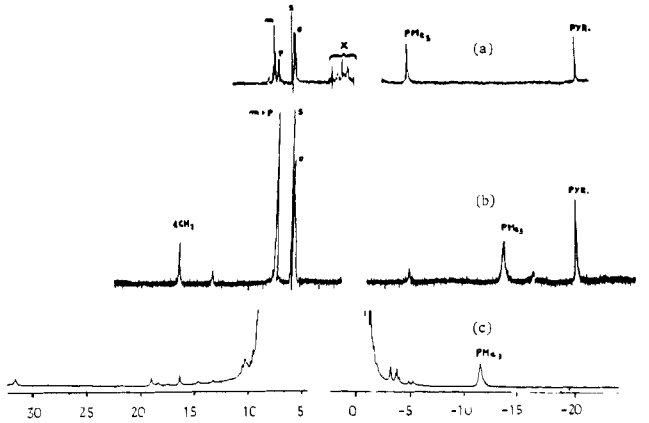

Figure 1. ^1H NMR spectra of (a) Fe(TPP)(PMe_3)$_2ClO_4$ (**1**) and (b) FeTPP(PMe_3)(1-MeIm)ClO_4 (**2**). The spectra were obtained in CD_2Cl_2 at 20 °C. Assignments of the various resonances are indicated; S marks the residual solvent peak, and X indicates impurity peaks. Tetramethylsilane was used as internal reference. (c) ^1H NMR spectrum of sperm whale metMbPMe_3 (3 mM protein solution in 0.1 M pH 7.4 phosphate/D_2O at 25 °C, DSS) taken from ref 3.

by consideration of the $P(CD_3)_3$ spectrum. Other information pertinent to assignments was gained from selective frequency coupling experiments and by consideration of relative intensities. The ^1H NMR spectra of Fe(DPDME)(PMe_2)$_2ClO_4$ and Fe(DPDME)(PMe_3)(1-MeIm)ClO_4 are also characteristic of low-spin ferric hemin complexes.[17] Most of the porphyrin resonances can be easily located and identified from their known spectral features.[17] The PMe_3 signal in both complexes is directly assigned through examination of the $(PCD_3)_3$ complex ($\delta = -5.5$ for the bis(phosphine) complex and $\delta = -13.2$ for the mixed-hexacoordinate complex).

In order to characterize the electronic structure of the phosphine iron porphyrin, analysis of the chemical shifts was made according to empirical methods.[15] The isotropic chemical shifts were calculated by using diamagnetic Fe(TPP)(PMe_3)$_2$ and Fe(TPP)(PMe_3)(1-MeIm) complexes as references.[7]

The geometric factor calculated values of the different porphyrin proton sites of Fe(TPP)(PMe_3)$_2ClO_4$, Fe(TPP)(PMe_3)(1-MeIm)ClO_4, and Fe(TPP)(PMe_3)(py)ClO_4 were first used to determine the corresponding dipolar shifts according to the method of La Mar and Walker.[18] This method depends on the fact that the meso-phenyl shifts are totally dipolar in origin.[19] Since the relative dipolar shifts for two protons in the same complex are given by their relative geometric factors, the dipolar contribution to the isotropic shift for PMe_3 can be obtained directly from the relative calculated geometric factors. With use of the structural data from our X-ray study of Fe(TPP)$PMe_2Ph)_2$,[7] the geometric factor for PMe_3 has been calculated with the reasonable assumption that the phosphine–iron geometry is essentially unaffected by phosphine substitution and change in the oxidation state $[(3\cos^2\theta - 1)/r^3 = 0.018\,37\ \text{A}^{-3}]$.[20] With the knowledge of both the isotropic and dipolar shifts (eq 1), the contact shifts are

$$\left(\frac{\Delta H}{H}\right)_{iso} = \left(\frac{\Delta H}{H}\right)_{dip} + \left(\frac{\Delta H}{H}\right)_{con} \quad (1)$$

obtained. The results are listed in Tables I–III (column A). Since the relative meso-aryl shifts in Fe(TPP)(PMe_3)$_2ClO_4$ clearly showed the presence of both contact and dipolar contributions in the meta positions (vide infra), ESR data were also used to estimate $(\Delta H/H)_{dip}$ in the two complexes Fe(TPP)(PMe_3)$_2ClO_4$ (**1**) and Fe(TPP)(PMe_3)(1-MeIm)ClO_4 (**2**). ESR measurements

(13) Walker, F. A.; Lo, M. W.; Ree, M. T. *J. Am. Chem. Soc.* **1976**, *98*, 5552.
(14) Ohya, T.; Morohoshi, H.; Sato, M. *Inorg. Chem.* **1984**, *23*, 1303.
(15) La Mar, G.; Walker, A. F. In *The Porphyrins*; Dolphin, D., Ed.; Academic: New York, 1978; Vol. 4, p 61.
(16) Preparated by addition of $P(OPh)_3$ to CD_3MgI in dibutyl ether.
(17) La Mar, G. N.; Chacko, V. P. *J. Am. Chem. Soc.* **1982**, *104*, 7002.
(18) La Mar, G. N.; Walker, F. A. *J. Am. Chem. Soc.* **1973**, *95*, 1782.
(19) Satterlee, J. D.; La Mar, G. N. *J. Am. Chem. Soc.* **1976**, *98*, 2804.
(20) The methyl group is not restricted from free rotation. Hence, the methyl proton geometric factor was calculated for a model[7] defined by the maximum angle $\theta_1 = 45°$ and the minimum angle $\theta_2 = 20°$, where $\theta = 0°$ when the Fe–H vector is perpendicular to the plane of the porphyrin ring.

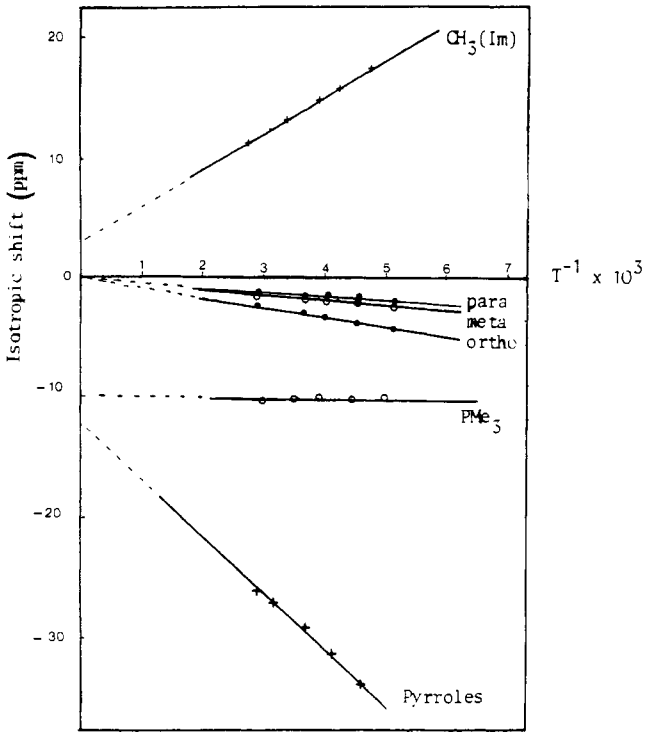

Figure 2. Plot of isotropic shift vs reciprocal temperature for Fe(TPP)(PMe_3)(1-MeIm)ClO_4 in CD_2Cl_2. Dotted lines are the high-temperature extrapolated lines for Curie behavior.

at 140 K yielded the following g values: for **1**, 2.687, 2.088, 1.680; for **2**, 2.890, 2.286, 1.542. The g values for **2** are in substantial agreement with those reported by Peisach,[21] Walker,[22] and La Mar.[17] We used the well-known equation[15]

$$\left(\frac{\Delta H}{H}\right)_{dip} = -\frac{\beta^2 S(S+1)}{9kT}(g_\parallel^2 - g_\perp^2)\left[\frac{3\cos^2\theta - 1}{r^3}\right] \quad (2)$$

which neglects the second-order Zeeman term. The effective axial field (a single pyrrole peak) permits the use of this equation with $g_\parallel = [{}^1/_2(g_{xx}^2) + {}^1/_2(g_{yy}^2)]^{1/2}$ and $g_\perp = g_{zz}$.

Also analysis of the curve in the Curie plot was made for the Fe(TPP)(PMe_3)(1-MeIm) complex. The temperature dependences of the isotropic shifts of the protons of **2** in CD_2Cl_2 are shown in Figure 2. The isotropic shifts vary linearly with T^{-1}, but the extrapolated lines do not pass through the origin at $T^{-1} = 0$.

Discussion

The room-temperature NMR data of (phosphine)iron(III) porphyrins are characteristic of the low-spin state of the ferric porphyrin system. All the phosphine complexes have pyrrole proton resonances between −19 and −21 ppm. These shifts are typical of iron(III) in a low-spin state for tetraarylporphyrin macrocycles.[15] This result is not unusual and can be attributed to the strong-field character of the phosphine ligand.

Analysis of the Porphyrin Shifts. The data in Table II indicate that the meso-phenyl shifts are totally dipolar in origin for the Fe(TPP)(PMe_3)(1-MeIm)ClO_4 complex. This conclusion is based on the observation that the dipolar shifts calculated from the relative geometric factors (column A) are in reasonable agreement with the dipolar shifts calculated by using the ESR data (column B). However, in the case of Fe(TPP)$(PMe_3)_2ClO_4$, inspection of the data in Table I reveals that the isotropic shifts are not totally dipolar in origin. In a previous analysis of the isotropic shifts of low-spin cyano complexes. La Mar et al. reported similar results.[24]

The large upfield pyrrole proton contact shifts agree with charge transfer from the porphyrin $3e_\pi$ orbitals to the d_{xz} and d_{yz} orbitals of the metal. This is expected for low-spin iron(III) derivatives. Nevertheless, the contact shift of the pyrrole H in Fe(TPP)-(PMe_3)(1-MeIm)$^+$ is smaller than that of the corresponding bis(phosphine) species Fe(TPP)$(PMe_3)_2^+$. This may reflect the $\sigma + \pi$ donating effect of imidazole[23] (vs the σ-donor and π-acceptor properties of phosphines), which reduces the tendency of porphyrin → Fe π back-bonding (the pyrrole H contact shift has been shown to reflect P→Fe π charge transfer).[24] The plot of the isotropic shifts vs T^{-1} for Fe(TPP)(PMe_3)(1-MeIm)ClO_4 in CD_2Cl_2 is linear for each type of proton as shown in Figure 2, but the extrapolated lines for pyrrole H and phosphine H do not pass through the origin at $T^{-1} = 0$.

Trimethylphosphine–Iron Bonding. The isotropic shift obtained in Table I for PMe_3 is slightly upfield. Inspection of the data suggests that the contact shift and the dipolar shift have similar magnitude but opposite signs. Thus, the coordination of an alkylphosphine to the metal center leads to a low-spin iron(III) porphyrin complex with unpaired spin density on the methyl group occurring from the occupied π-symmetry d_{xz} and d_{yz} orbitals. A dramatic change is observed with Fe(TPP)(PMe_3)(1-MeIm)ClO_4. In comparison to that in the bis(phosphine) species, the PMe_3 proton signal is at stronger field (~10 ppm), implying that the contact shift dominates. This effect favors the interpretation that spin transfer in both species involves iron→PMe_3 π charge transfer. This mechanism would be enhanced by the presence of an axial imidazole acting primarily as a π donor. The role of such π-bonding has been recently demonstrated by Traylor et al.[23] on the basis of the effect of an axial imidazole on the in-plane asymmetry in natural porphyrin complexes. Similar conclusions have also been reached by La Mar et al.[17] In this case, deprotonation of an axial imidazole leads to hyperfine changes for porphyrin substituents that reflect primarily a decrease in ligand→metal π charge transfer. Moreover, while separation of dipolar and contact shifts for the natural porphyrins has not been made, the similar shift changes observed with PMe_3 between the symmetric and the mixed-ligated complexes suggest that the same spin-transfer mechanism may apply to the natural complexes. Finally, it should be stressed that a related study involving a series of trivalent phosphorus ligand complexes of cobalt(II) tetraphenylporphyrin that have an odd electron isolated in a σ molecular orbital has been previously reported by Wayland et al.[25]

PMe_3 as a Potential Protein Probe. From consideration of the chemical shift of the axial trimethylphosphine protons in the present complexes, it seems reasonable to expect that PMe_3 in low-spin ferric hemoproteins should resonate upfield of the diamagnetic region irrespective of the nature of the protein. Our results on metMbPMe_3 (Figure 1c) and metHbPMe_3 have already confirmed part of this hypothesis.[3] Therefore, the large isotropic shift of PMe_3 may prove useful for a more accurate description of the active site of cytochrome P450. Such work is currently under way.

(21) Peisach, J.; Blumberg, W. E.; Adler, A. D. *Ann. N.Y. Acad. Sci.* **1973**, *206*, 310.
(22) Walker, F. A.; Reis, D.; Balke, V. L. *J. Am. Chem. Soc.* **1984**, *106*, 6888.
(23) Traylor, T. G.; Berzini, A. P. *J. Am. Chem. Soc.* **1980**, *102*, 2844.
(24) La Mar, G. N.; Del Gaudio, J.; Frye, J. S. *Biochim. Biophys. Acta* **1977**, *498*, 422.
(25) Wayland, B. B.; Abd-Elmageed, M. E. *J. Am. Chem. Soc.* **1974**, *96*, 4809.